Differential effects of wheat bran antioxidants on the growth dynamics of human cancer cells

by

Md Sharifur Rahman

B.Sc., Bangladesh Agricultural University, 2015
MS, Bangladesh Agricultural University, 2017

A THESIS

submitted in partial fulfillment of the requirements for the degree

MASTER OF SCIENCE

Card and Melinda Heiwig Department of Biological and Agricultural Engineering
Carl R. Ice College of Engineering

KANSAS STATE UNIVERSITY
Manhattan, Kansas

2025

Approved by:

Major Professor
Dr. Donghai Wang

Copyright

Abstract

Wheat bran, rich in phenolic compounds like ferulic acid, possesses notable antioxidant properties that may contribute to cancer treatment strategies. This study examined the effects of hydrolyzed arabinoxylan oligomers (HAO) linked with ferulic acid from hard wheat bran on three human cancer cell lines: colon cancer (SW480), liver cancer (HepG2), and cervical cancer (HeLa). Cells were cultured in a three-dimensional (3D) PGmatrix and exposed to varying concentrations (100, 500, and 1000 μg/ml) of wheat bran extracts (WBE). Results showed that WBE inhibited growth of SW480 cells, significantly reducing spheroid expansion and promoting dehydration. In contrast, HepG2 cells exhibited increased growth under WBE treatment, suggesting a non-toxic, growth-enhancing effect. No significant changes were observed in HeLa cell growth, with cell viability remaining high across all treatments. These findings highlight the selective influence of WBE on cancer cell behavior, underscoring its potential for targeted, personalized cancer therapies. This study provides valuable insights into the application of antioxidant-rich compounds for modulating specific cancer cell dynamics, paving the way for novel therapeutic approaches.

Table of Contents

List of Figures

List of Tables

Acknowledgements

I would like to express my heartfelt gratitude to everyone who supported me throughout the completion of this thesis. This work would not have been possible without the guidance, encouragement, and contributions of many individuals, as well as the invaluable resources provided by Kansas State University.

My deepest thanks go to my advisor, Dr. Susan Sun, for her unwavering support, insightful feedback, and vast expertise. Her dedication and passion for research have been a constant source of inspiration, and I am truly grateful for the opportunities and challenges she provided.

I also wish to thank my Major Professor Dr. Donghai Wang, and Committee Member Dr. Weiqun Wang, for their thoughtful suggestions, which greatly improved the quality and depth of this work. I am additionally grateful to Dr. Mark Wilkins and Dr. Aleksey Sheshukov for their guidance and assistance.

I am deeply thankful to the Card and Melinda Heiwig Department of Biological and Agricultural Engineering for their support and for providing the research facilities throughout my master's program. Special thanks to Kansas State Veterinary and Diagnostic Laboratories (KSVDL) for their help with the H&E staining.

A special note of thanks to Dr. Guangyan Qi and Dr. Quan Li, with whom I shared invaluable lab experiences. Their camaraderie and stimulating discussions were essential to the success of my projects.

I am forever grateful to my family in Bangladesh—my parents, Golam Mostafa and Jahanara Pervin, and my siblings, Md Arifur Rahman and Monira Akter—for their unwavering love and belief in me. My son, Ariz Rahman, has been a constant source of inspiration. Above all, I thank my wife, Aysha Mobaswera, whose sacrifices, encouragement, and understanding have

been my greatest comfort and motivation. This achievement is dedicated to all of you, and I strive to make you proud. I am also thankful to Bangladeshi Student Association (BSA) at K-state for their support and friendliness.

To all who have supported me on this journey, your encouragement, in all its forms, has been deeply appreciated. This thesis is as much yours as mine is. Thank you!

Dedication

To Dr. Susan Sun, for your guidance and mentorship throughout this process, and my parents, whose spirit continues to inspire me.

Preface

The exploration of natural compounds for therapeutic applications has always fascinated me, particularly their potential in addressing complex diseases like cancer. This thesis, rooted in my passion for cancer biology, investigates the effects of wheat bran-derived antioxidants on specific cancer cell lines in innovative 3D culture systems. The journey of this research was enriched by the guidance of Dr. Susan Sun. I hope this work contributes to advancing personalized cancer therapies and inspires future studies in the field of antioxidant-based interventions.

Md Sharifur Rahman

April 2025

Chapter 1 - Introduction

Natural antioxidants, particularly phenolics and bioactive compounds derived from dietary sources, have gained considerable attention for their anti-inflammatory, anti-cancer, and anti-aging properties [1]. Phenolic-rich byproducts such as rice bran, grape pomace, apple peel, have been stabilized and utilized as low-cost materials to extract various valuable compounds for nutraceuticals, dietary supplements, and functional food formulations [2]. Wheat-based materials represent a cost-effective and abundant source of antioxidants [3]. Among wheat components, wheat bran, a byproduct of the flour milling process, contains the highest concentration of phenolic compounds, known for their potent in vitro antioxidant activity and their ability to prevent low-density lipoprotein oxidation and DNA damage, can be utilized as a functional food and dietary intervention [3,4]. Arabinoxylan (AX), a primary constituent of wheat bran, provides several health benefits, including antioxidant effects, modulation of gut microbiota, production of short-chain fatty acids, and anti-cancer properties [3,5]. AX's antioxidant potential primarily stems from its attached phenolic acids, which stabilize free radicals through resonance [6,7]. However, the polymeric structure of AX can obscure these phenolic acids, reducing its antioxidant efficacy. Hydrolyzing AX into xylo-oligosaccharides (XOS) via xylanase is thought to enhance antioxidant capacity compared to intact wheat bran [3]. Previous studies evaluating whole wheat bran may not accurately reflect the antioxidant potency of XOS, as other components such as fat, starch, and protein can confound the results [3].

Antioxidants play a vital role in neutralizing reactive oxygen species (ROS)—highly reactive molecules that induce oxidative stress and damage essential cellular components, including DNA, lipids, and proteins [1,5,8]. The role of oxidative stress in cancer progression is well-established, as excessive ROS can lead to genetic mutations, uncontrolled cell proliferation,

and metastasis [9–11]. This has led to growing interest in the therapeutic potential of wheat bran antioxidants (WBA) to modulate cancer cell growth. Although numerous studies have documented the antiproliferative effects of dietary antioxidants on various cancer cell lines, the specific influence of wheat bran XOS on 3D-cultured cancer cells remains largely unexplored [1,12]. This study aims to address that gap by investigating the effects of WBE on three cancer cell lines—colon cancer (SW480), liver cancer (HepG2), and cervical cancer (HeLa).

Colorectal cancer, one of the most common cancer types globally, is represented by SW480 cell line, derived from a primary adenocarcinoma of the colon and commonly used to model colorectal cancer progression in vitro [13,14]. Studies show that dietary antioxidants can inhibit colorectal cancer cell growth by modulating signaling pathways such as Wnt/β-catenin and PI3K/AKT, which are crucial for cell proliferation and survival [13,14]. For instance, antioxidants like quercetin and resveratrol induce apoptosis and inhibit colon cancer cell proliferation via ROS-mediated mechanisms [15]. Given WBE's high antioxidant capacity, we hypothesize that it may exert similar growth-suppressive effects on SW480 cells by modulating ROS levels and related pathways. Additionally, liver cancer, represented by the HepG2 cell line, is the third leading cause of cancer-related deaths, particularly due to its aggressive nature and resistance to conventional treatments [16]. Previous research highlights the role of antioxidants in promoting liver cell survival while reducing tumor growth, suggesting that WBE may support healthy liver cell function while inhibiting malignant transformation [17,18]. For cervical cancer, HeLa cells are a widely recognized model, with studies indicating that antioxidants may disrupt cancer progression by targeting ROS-driven cellular mechanisms [19,20]. Although antioxidants like vitamin C and polyphenols have been examined in cervical cancer studies, their effects in a 3D culture

environment—which closely mimics the tumor microenvironment—remains underexplored [20,21].

This study incorporates a 3D embedded culture system using a 0.5% PGmatrix-Spheroids (PGS) matrix to provide a physiologically relevant assessment of how WBE affects cancer cell growth and spheroid formation in SW480, HepG2, and HeLa cell lines. Since 3D cultures better simulate the *in vivo* environment, this approach enables more accurate observations of cell-cell and cell-matrix interactions, which are essential for understanding cancer biology [22,23]. Furthermore, 3D systems establish gradients of oxygen, nutrients, and metabolites, which are critical for exploring mechanisms such as hypoxia, metabolic adaptation, and chemoresistance [24]. Through a comprehensive evaluation of WBE's cytotoxic effects on SW480, HepG2, and HeLa cancer cell lines, this research aims to offer new insights into the role of antioxidants in cancer therapy and deepen our understanding of how antioxidants impact cancer cell biology.

Chapter 2 - Materials and Methods

2.1. WBA extraction

Xylo-oligosaccharides linked with ferulic acid were extracted from hard red winter wheat bran (protein content: 16.8%), sourced from the Hal Ross Flour Mill in Manhattan, Kansas, following the method outlined by Cheng et al. (2024) [3]. The extraction process began with defatting the bran, where 4 mL of hexane per gram of bran was used for a 1-hour extraction. The defatted bran was then air-dried in a fume hood. Subsequently, destarching was carried out using α-amylase (500 U/mg) at pH 6, followed by deproteinization with Alcalase (0.8 U/g) at pH 7.5 for 30 minutes at an optimal temperature of 60 ^{o}C. After deproteinization, the resulting protein hydrolysate was heat-inactivated by boiling. Xylanase was added to the pretreated bran in 20 mM sodium acetate buffer (pH 5.5), and the mixture was incubated at 50 ^{o}C for 12 hours. Following incubation, the mixture was centrifuged at 8000 × g for 15 minutes to separate the supernatant, which was then dialyzed at 4 ^{o}C for three days before being lyophilized to yield the xylo-oligosaccharide (XOS).

2.2. Cell cultures

2.2.1. Cell lines

Human colorectal carcinoma SW480, human hepatocellular carcinoma HepG2 (HB-8065) and human cervical carcinoma HeLa cell lines were purchased from American Type Culture Collection (ATCC) (Manassas, VA, USA).

2.2.2. Cell culture condition

The PGmatrix Spheroids (PGS) kit (PepGel LLC, Winston Salem, NC, USA) was used according to the manufacturer's user guide. Briefly, cell suspension at a desirable seeding density in selected medium was initially mixed with PGworks (PepGel LLC). PGS was then added to this mixture and thoroughly blended. The resulting cell mixture was dispensed into a 24-well plate at 500 μL per well and incubated at 37 °C for 30 minutes to form a hydrogel. According to our preliminary testing, 0.5% PGS showed desirable gel strength to hold the cell spheroids suspended (no precipitation). Following gelation, the target medium was gently added to feed the cells. Then cells were fed as needed in the following days as described in each cell line culture protocols in section 2.4.

2.3. Cell spheroids harvesting and dissociation

Cancer spheroids were harvested from the 3D embedded culture following the manufacturer's guidelines (PepGel LLC). Briefly, to disrupt the gel, the gel and medium were pipetted 6–8 times, then transferred to a conical tube. To dilute the solution for separation, 20 volumes of DPBS without calcium were added. The mixture was centrifuged at 500×g at 24 ^{o}C for 5 minutes. After centrifugation, the supernatant was discarded, and cancer spheroid pellets were collected from the bottom of the tube. These spheroids were used for fixation and staining analysis.

For cell passage or cryopreservation, these spheroids were dissociated into single cells by incubating with 1 mL/well of trypsin EDTA 0.25% (5X) at 37 ^{o}C. Once sufficient cell dissociation was observed under a microscope, the trypsinization was stopped by adding culture medium and the dissociation time was recorded. Cells were washed and centrifuged for passage or cryopreservation as well as analysis or applications as needed.

2.4. Growth performance of cancer cells with WBE induction

2.4.1. SW480 3D culture, WBE induction, and harvesting

SW480 cells were cultured under 3D embedded conditions in 0.5% PGS using DMEM complete medium (DMEM + 10% FBS + 1% P/S) as described in section 2.2. In one well of a 24-well plate, a solution containing 2×10^4 single cells in 240 µl, 10 µl PGworks, and 250 µl 1% PGS were added. On day 3, 1 ml of medium was carefully aspirated without disturbing the cells and 1.5 ml of fresh medium was added along with the required volume of WBE solution as specified in Table 1. Cells were harvested on day 7 according to the procedure described in section 2.3.

2.4.2. HepG2 culture, WBE induction, and harvesting

HepG2 cells were cultured under 3D embedded condition in 0.5% PGS using DMEM complete medium following the procedure described in section 2.2. In one well of a 24-well plate, a solution containing 4×10^4 single cells in 240 µl, 10 µl PGworks, and 250 µl of 1% PGS was added. On day 3, 1 ml of medium was carefully removed without disturbing the cells, and 1.5 ml of fresh medium was added along with the required volume of WBE solution as specified in Table 2.1. Cells were harvested on day 7 following the procedure in Section 2.3.

2.4.3. HeLa culture, WBE induction, and harvesting

HeLa cells were cultured in the 3D embedded condition in 0.5% PGS using DMEM complete medium following the procedure described in section 2.2. In one well of a 24-well plate, a solution containing 4×10^4 single cells in 240 µl, 10 µl PGworks, and 250 µl of 1% PGS was added. On day 4, 1 ml of medium was carefully removed without disturbing the cells, and 1.5 ml of fresh medium was added along with the required volume of WBE solution as specified in Table 2.1. Cells were harvested on day 8 following the procedure in Section 2.3.

Table 2.1. WBE concentration, the volume of WBE induction, and the volume of fresh medium addition in the 3D embedded condition in a 24-well plate (24-WP).

SN	WBE concentration (µg/ml cell suspension)[1]	In 24-WP	2% WBE solution and fresh medium addition
01	100	200 µg/2 ml/well	10 ul 2% WBE solution with 1500 ul fresh media
02	500	1000 µg/2 ml/well	50 ul 2% WBE solution with 1500 ul fresh media
03	1000	2000 µg/2 ml/well	100 ul 2% WBE solution with 1500 ul fresh media

[1]To select the concentration of WBE, we aimed to encompass a range from low to high doses to observe potential dose-dependent effects. Previous studies have employed varying concentrations of wheat bran extracts to evaluate their anticancer properties [25,26].

2.5 Cell morphology and image analysis

Bright-field and fluorescence imaging were conducted using an Axio Vert A1 inverted microscope (Carl Zeiss Microscopy, Germany). Image processing and analysis were performed using FIJI-ImageJ software [27].

2.6. Cell count and viability measurement

Following the cell retrieval procedures outlined previously, cell count, and viability were assessed using Auto2000 Cellometer (Nexcelom Bioscience LLC, Lawrence, MA, USA) with an

acridine orange/propidium iodide (AO/PI) assay from Nexcelom Bioscience. A 20 µL aliquot of well-suspended cell solution was mixed with 20 µL of AO/PI reagent. The cellometer programmed for bright-field and dual-fluorescence imaging, detected live and dead cells: live cells fluoresced green, while apoptotic cells with early membrane damage fluoresced orange. The cellometer calculated and reported cell count, diameter, viability, and concentration. Fold change was determined by dividing the total number of harvested cells by the initial seeding number and viability was calculated by dividing the total number of live cells by the total number of harvested cells.

2.7. Hematoxylin and eosin (H&E) staining

Cancer cell spheroids were fixed overnight in 10% neutral buffered formalin, washed with DPBS supplemented with Ca2+/Mg2+ (Sigma), and subsequently embedded in 1% agar (Sigma–Aldrich) solution cooled to approximately 60 °C. The agar-embedded samples were then processed and embedded in a paraffin. These embedded samples were sectioned, mounted onto glass slides, dewaxed, and subjected to staining with hematoxylin and eosin, and imaging. Image processing was performed using FIJI ImageJ version 1.54k [27].

2.8. Statistical analysis

All statistical analyses were conducted using Microsoft Excel and Minitab, with results presented as mean ± standard deviation (SD). Significance was evaluated using one-way ANOVA with Tukey HSD multiple comparisons. Statistical significance was set at $p \leq 0.05$. All experiments were performed in triplicate ($n = 3$) to ensure reproducibility of the results.

Chapter 3 - Results

3.1. WBE alleviates SW480's growth performance

SW480 cells formed spheroids in 3D PGS system, resembling a cluster of grapes, with well-hydrated, circularly shaped cells loosely arranged without forming any distinct hollow structures or specific cellular organization within the spheroids. In contrast, WBE treatment significantly altered the morphology of the SW480 cells. WBE-treated spheroids appeared more like clusters of dehydrated, squished grape raisins. The cells exhibited a more compressed and parched appearance, with the spheroids adopting a more compact circular shape. The degree of dehydration increased with concentrations of WBE. Consequently, the spheroid's diameter decreased with WBE concentration: control spheroids had a diameter of approximately 40-60 μm, while 1000 μg/ml WBE-treated spheroids measured about 30 to 50 μm in diameter. Despite these morphological changes, no precipitation was observed in any treatment conditions. However, a noticeable reduction in spheroid count was observed at higher WBE concentrations (Figure 3.1).

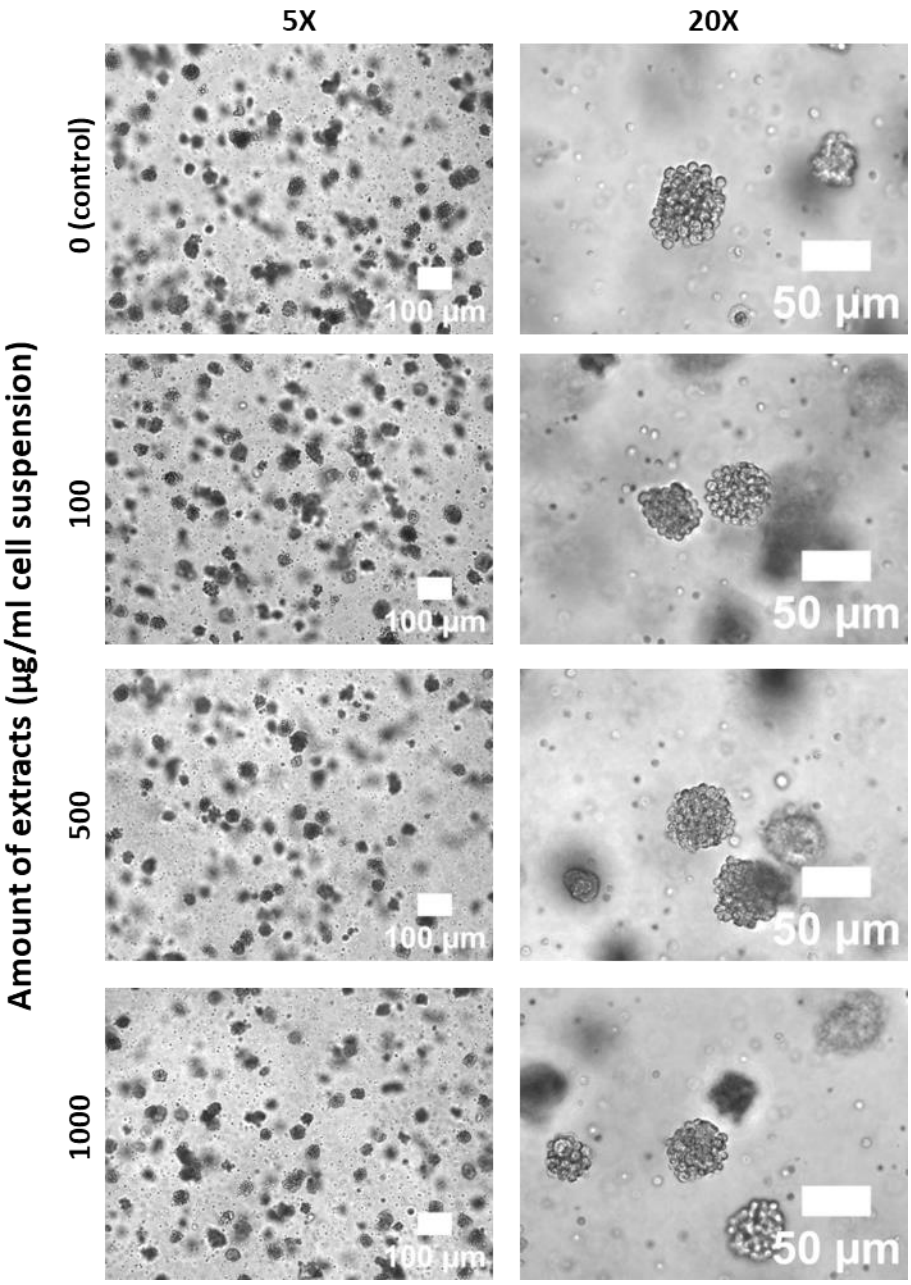

Figure 3.1 Cell morphology of SW480. The scale bars are 100 and 50 µm, the resolutions are 5X and 20X. Cells were cultured in 3D embedded conditions using PGS (0.5%) in 24 well plates. WBE was induced on day 3 and the cell was harvested on day 7. The cell spheroids shown in the figure are also on day 7.

On day 7, cells were harvested and treated with 0.25% trypsin-EDTA (5X) to dissociate into single cells, and dissociation times were recorded to evaluate WBE's impact on cell detachment. Dissociation times increased significantly with higher WBE concentrations, with control and 1000 µg/ml WBE-treated SW480 cells showing times of 15±0.82 and 19.75±0.96 minutes, respectively. However, no effect on dissociation time was observed at lower concentrations, such as 100 µg/ml (Figure 3.2).

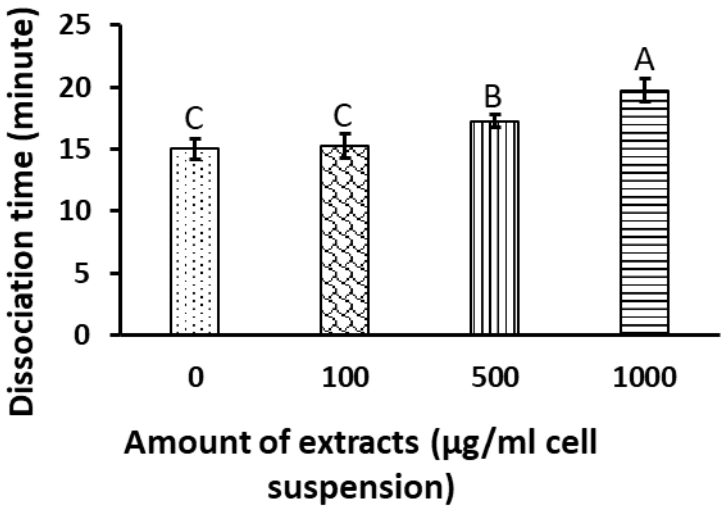

Figure 3.2 Cells dissociation time with trypsin EDTA 0.25% at 37 ^{o}C. Data are shown in means ± SD of three independent biological replicates (n = 3). $p < 0.05$. The means that do not share a letter are significantly different.

The effects of WBE on cell fold expansion and viability were assessed after a 4-days exposure period. Cell viability remained relatively stable up to 500 µg/ml WBE but significantly decreased at 1000 µg/ml, although it still exceeded 95%, indicating a strong survival rate. In terms of cell growth, WBE-treated cells exhibited markedly reduced fold expansion compared to the

control group, with a clear reduction corresponding to each increase in WBE concentration. The growth rate for control cells was 22.33±1.31, while cells treated with 1000 µg WBE showed approximately 40% less growth, demonstrating that WBE exerts a toxic effect on SW480 colon cancer cells (Figure 3.3). These findings also suggest that WBE possesses growth-suppressing effects in SW480 cells, highlighting its potential as a candidate for colon cancer treatment.

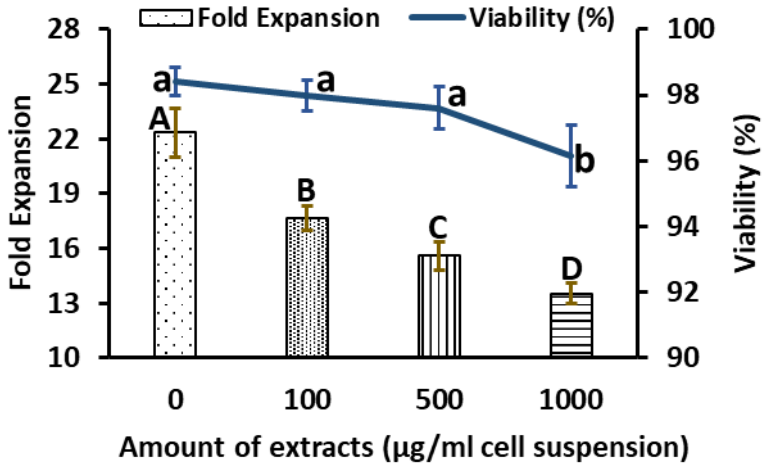

Figure 3.3 Fold expansion and viability of SW480. Data are shown in means ± SD of three independent bio-logical replicates (n = 3). $p < 0.05$. The means that do not share a letter are significantly different. Cells were cultured in 3D embedded conditions using PGS (0.5%) in 24 well plates. WBE was induced on day 3 and the cell was harvested and counted on day 7.

SW480 cells were subjected to H&E staining to assess cell pattern, shape, and structure within the spheroids. Due to significant cell dissociation during sample preparation, fewer spheroids were available for imaging, especially for control. Structural differences were observed between the control and WBE-treated SW480 cells. Control SW480 spheroids exhibited hyperchromatic nuclei, and a potentially higher nuclear-to-cytoplasmic ratio compared to WBE-

treated cells. Nucleus size was decreased with an increase in WBE concentration, along with a reduction in individual cell diameter, resulting in greater intercellular distances within the WBE-treated spheroids (Figure 3.4).

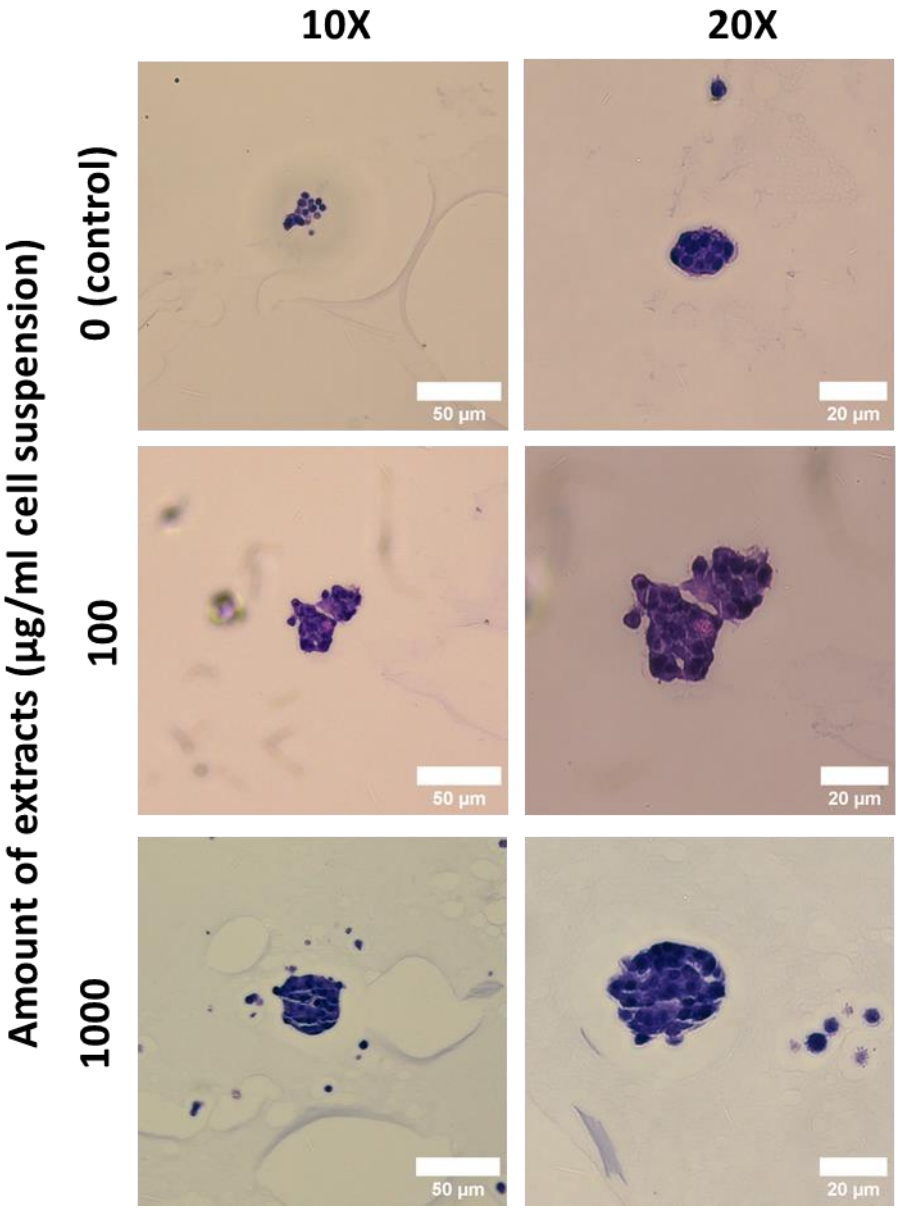

Figure 3.4 Cell spheroid images of H&E stained WS480. The scale bars are 50 and 20 µm, the resolutions are 10X and 20X. Cells were cultured in 3D embedded conditions using PGS (0.5%)

in 24 well plates. WBE was induced on day 3 and the cell was harvested on day 7. Then, cells were fixed and processed for H&E staining.

3.2. WBE accelerates HepG2's growth performance

Like WS480, HepG2 cells formed spheroids with varying sizes observed within the same treatment group. However, the cells within the spheroids were tightly packed, making individual cells indistinguishable, and there was no specific arrangement of cells. WBE treatment did not significantly alter HepG2 cell morphology; however, an increase in spheroid size was observed in a subset of spheroids at higher WBE concentrations (Figure 3.5). On day 7, the spheroids were harvested and then treated with trypsin-EDTA 0.25% (5X) to dissociate them into single cells. WBE was found to influence dissociation time in HepG2 cells, with increased dissociation time correlating with higher WBE concentrations; for instance, control and 1000 μg/ml HepG2 cells required 20±0.82 and 32±1.64 minutes, respectively, for dissociation. However, lower WBE concentrations, such as 100 μg/ml, did not affect dissociation time (Figure 3.6).

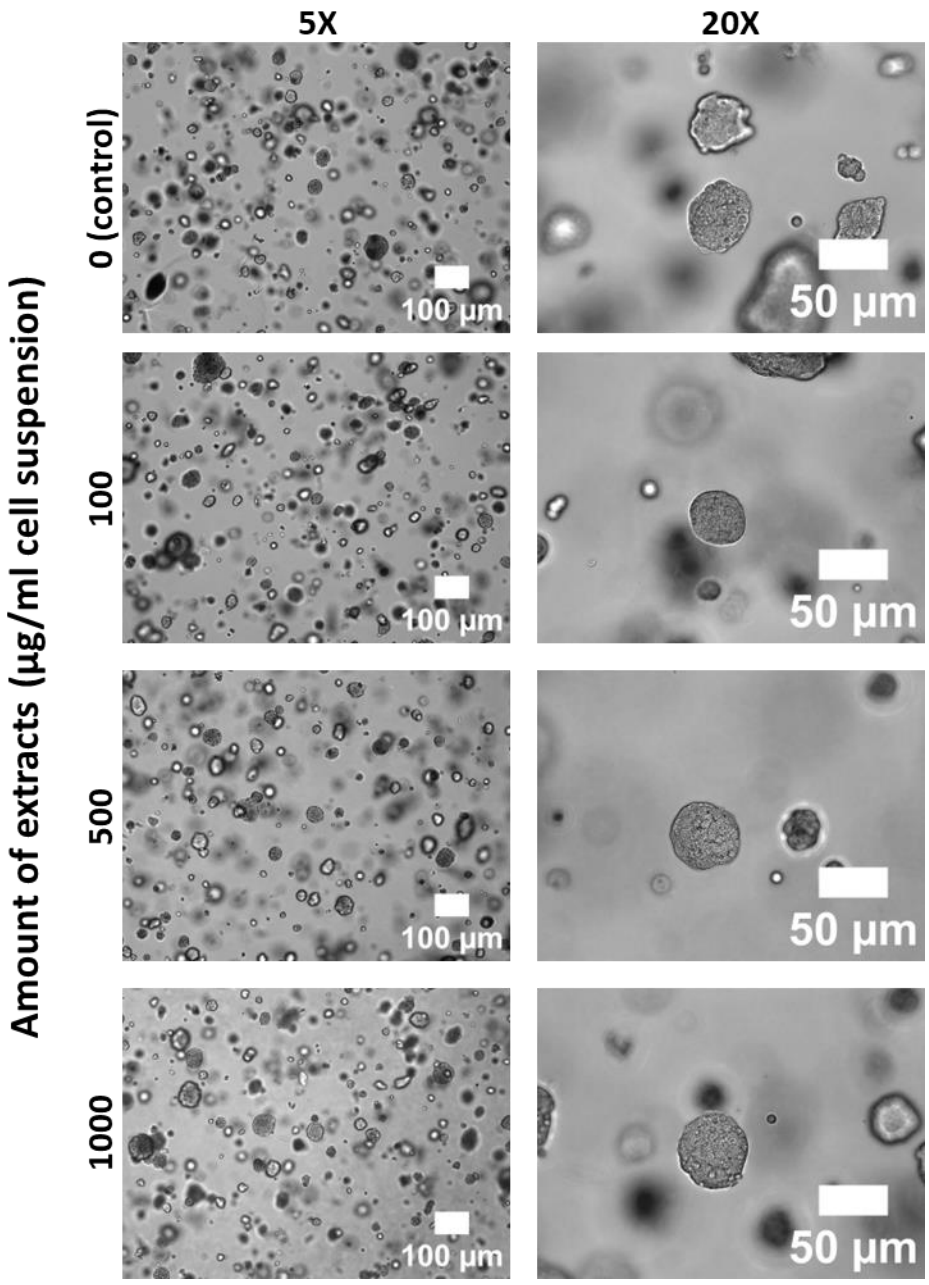

Figure 3.5 Cell morphology of HepG2. The scale bars are 100 and 50 µm, the resolutions are 5X and 20X. Cells were cultured in 3D embedded conditions using PGS (0.5%) in 24 well plates. WBE were induced on day 3 and the cell was harvested on day 7. The cell spheroids shown in the figure are also on day 7.

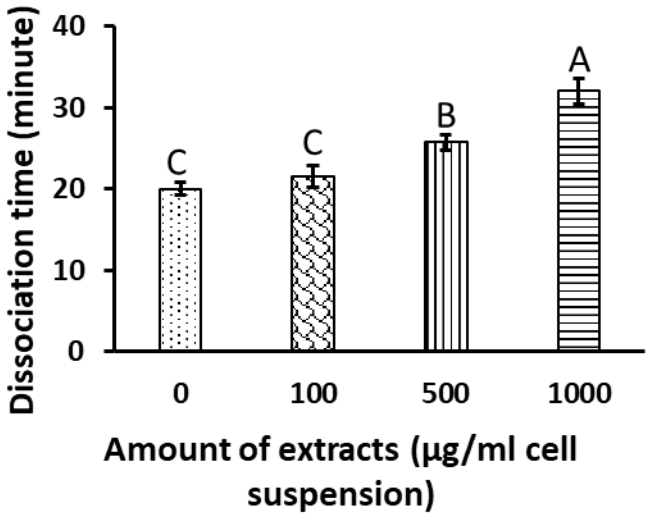

Figure 3.6 HepG2 cell dissociation time with trypsin EDTA 0.25% at 37 ^{o}C. Data are shown in means ± SD of three independent biological replicates (n = 3). $p < 0.05$. The means that do not share a letter are significantly different.

Cell fold expansion and viability were assessed after a 4-day exposure to WBE. Cell viability remained consistently around 95% across all treatments, with no significant differences between control and WBE-treated cells. In contrast, cells treated with 1000 µg of WBE showed significantly higher fold expansion compared to the control, with growth increasing in line with WBE concentration. Control cells had a growth rate of 13.42±1.15, while cells treated with 1000 µg WBE exhibited approximately 30% higher growth, suggesting that WBE positively affects HepG2 liver cancer cells (Figure 3.7). These findings indicate that WBE promotes HepG2 cell growth without exhibiting toxicity, suggesting potential antioxidant-driven, growth-enhancing properties.

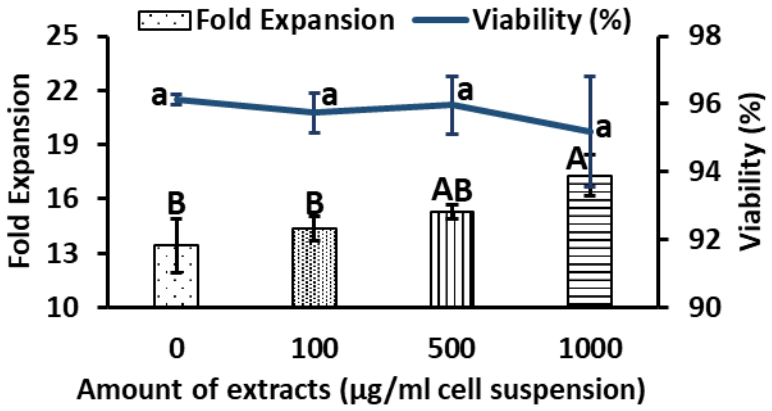

Figure 3.7 Fold expansion and viability of HepG2. Data are shown in means ± SD of three independent biological replicates (n = 3). $p < 0.05$. The means that do not share a letter are significantly different. Cells were cultured in 3D embedded conditions using PGS (0.5%) in 24 well plates. WBE was induced on day 3 and the cell was harvested and counted on day 7.

Additionally, H&E staining was performed on HepG2 spheroids to examine cellular morphology, structural organization, and spatial arrangement. Control and WBE-treated HepG2 spheroids were irregular in shape and cells were evenly distributed without forming any pattern. There was no significant difference between the control and treated cells, both cells looked well-hydrated and had a high nuclear-to-cytoplasm ratio (Figure 3.8).

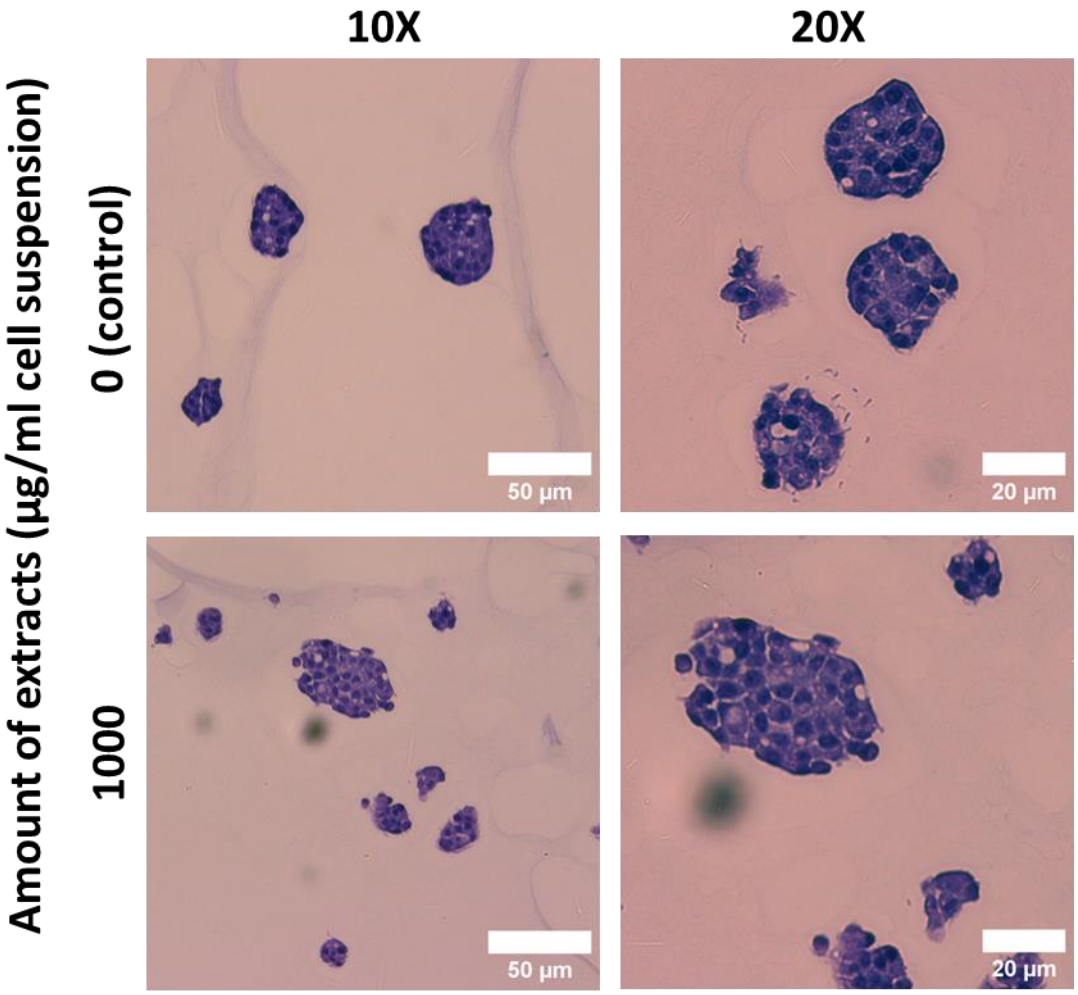

Figure 3.8 Cell spheroid images of H&E stained HepG2. The scale bars are 50 and 20 µm, the resolutions are 10X and 20X. Cells were cultured in 3D embedded conditions using PGS (0.5%) in 24 well plates. WBE was induced on day 3 and the cell was harvested on day 7. Then, cell was fixed and processed for H&E staining.

3.3. WBE does not interfere with HeLa's growth performance

Hela cells formed spheroids in 3D PGS embedded condition, though some exhibited slight deformations. Cells within the spheroids were densely packed, making individual cells indistinguishable, with no specific cellular arrangement. WBE treatment did not significantly affect the morphology of the HeLa spheroids, and no cell precipitation was observed in either treated or untreated groups (Figure 3.9). During harvesting, dissociation times were also recorded to evaluate the impact of WBE on cell dissociation time. WBE had no noticeable effects on HeLa cell spheroid dissociation times; control and 1000 μg/ml HeLa cells had dissociation times of 6±0.81 and 7.75±1.25 minutes, respectively (Figure 3.10).

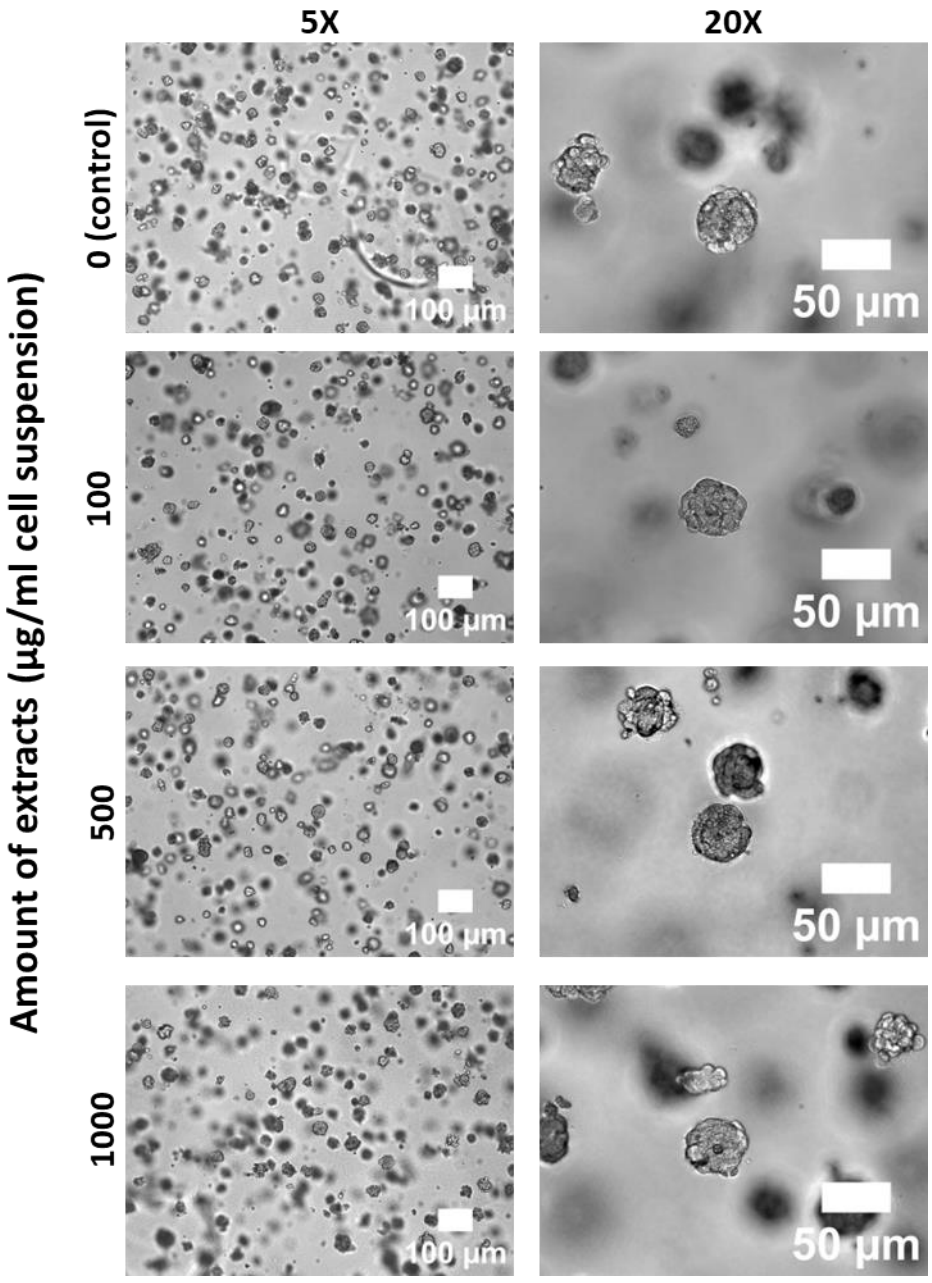

Figure 3.9 Cell morphology of HeLa. The scale bars are 100 and 50 µm, the resolutions are 5X and 20X. Cells were cultured in 3D embedded conditions using PGS (0.5%) in 24 well plates. WBE was induced on day 4 and the cell was harvested on day 8. The cell spheroids shown in the figure are also on day 8.

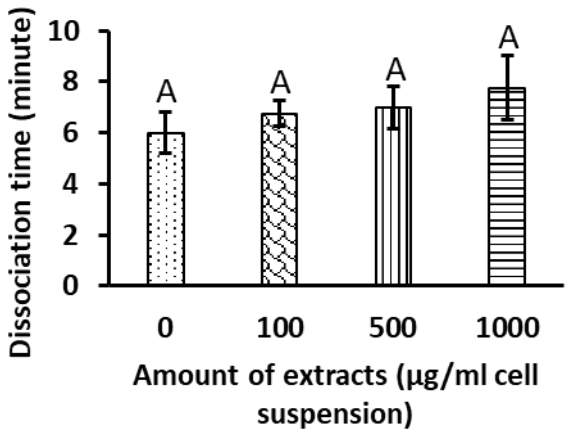

Figure 3.10 Cells dissociation time with trypsin EDTA 0.25% at 37 ^{o}C. Data are shown in means ± SD of three independent biological replicates (n = 3). $p < 0.05$. The means that do not share a letter are significantly different.

Cell fold expansion and viability were assessed after a 4-day exposure to WBE. Viability remained consistently around 97% across all treatments, with no significant differences between control and WBE-treated cells. Although there was a slight increase in fold expansion in the WBE-treated group, this increase was not statistically significant compared to the control (Figure 3.11). HeLa may activate cellular pathways (e.g., Nrf2 signaling) that increase the expression of detoxifying enzymes and protective molecules [28]. This suggests that WBE does not affect the growth of cervical cancer HeLa cells and does not exhibit any toxic effects on them.

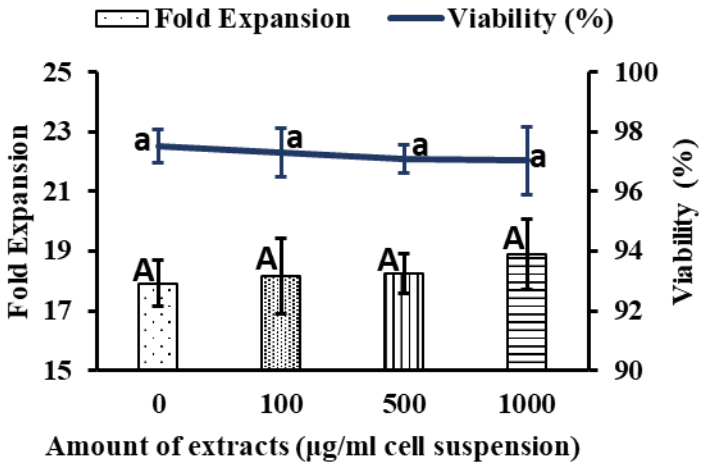

Figure 3.11 Fold expansion and viability of HeLa. Data are shown in means ± SD of three independent biological replicates (n = 3). $p < 0.05$. The means that do not share a letter are significantly different. Cells were cultured in 3D embedded conditions using PGS (0.5%) in 24 well plates. WBE was induced on day 4 and the cell was harvested and counted on day 8.

HeLa cells were also stained with H&E to examine cell spheroids anatomy. Cells adhered to one another with small gaps between them in the spheroids, with no distinct arrangement. Both control and WBE-treated cells displayed hyperchromatic nuclei and potentially higher nuclear-to-cytoplasmic ratios. Therefore, there were no significant differences in cellular morphology between WBE-treated and untreated cells (Figure 3.12).

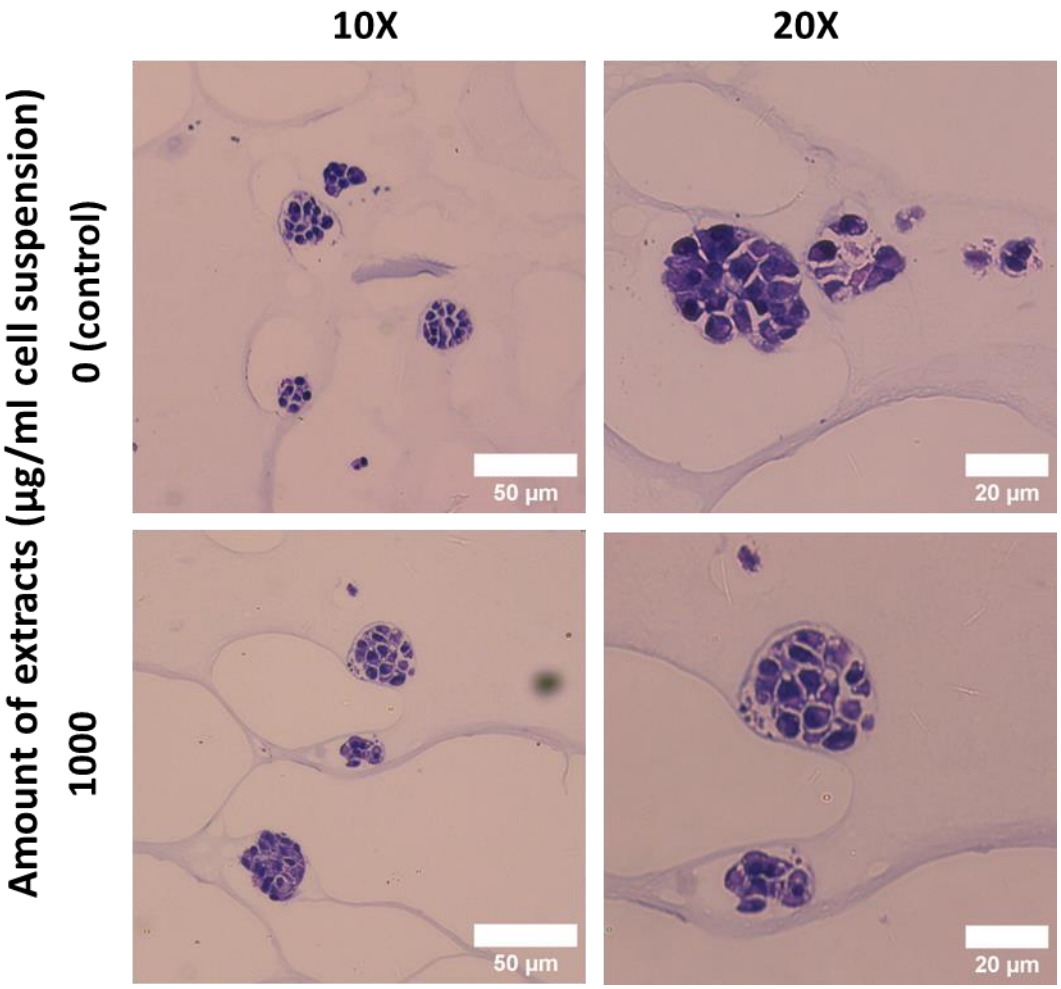

Figure 3.12 Cell spheroid images of H&E stained HeLa. The scale bars are 50 and 20 µm, the resolutions are 10X and 20X. Cells were cultured in 3D embedded conditions using PGS (0.5%) in 24 well plates. WBE was induced on day 4 and the cell was harvested on day 8. Then, cell was fixed and processed for H&E staining.

Chapter 4 - Discussion

WBE was tested on three human cancer cell lines to assess its cytotoxic effects. In SW480 cells, the observed morphological alterations, such as cell shrinkage and membrane blebbing, are likely linked to WBA-induced oxidative stress and disruption of intra-cellular water balance [29]. Previous studies have demonstrated that natural antioxidants, such as those derived from wheat bran, sorghum bran, coffee grounds, and rice bran, can generate ROS, leading to oxidative stress in cancer cells [30–32]. This stress triggers morphological changes, including cellular dehydration, possibly due to damage to the cell membrane or cytoskeletal components, impairing the ability to regulate osmotic pressure [33,34]. Increased dissociation times in WBE-treated cells may reflect reduced structural integrity and cytoskeletal reorganization. The reduced nuclear-cytoplasmic ratio and condensed cytoskeleton observed in these cells further suggest apoptosis pathway activation [35]. WBE's ability to suppress fold expansion aligns with findings from other polyphenolic antioxidants, which have been shown to disrupt cell cycle progression and induce apoptosis in cancer cells [30–33]. ROS generated by antioxidants can damage DNA, impair mitochondrial function, and activate pro-apoptotic signaling, contributing to cell death [29,32,34,35]. WBA may modulate the Wnt/β-catenin signaling pathway, which is often aberrantly activated in colorectal cancer. Phenolic compounds present in WBE, such as ferulic acid can influence this pathway by promoting the degradation of β-catenin, thereby reducing its nuclear translocation and subsequent transcriptional activation of oncogenes like c-Myc and Cyclin D1 [36], resulting the inhibition of cell proliferation. These findings suggest WBE holds potential as a therapeutic agent for colon cancer, warranting further exploration of its molecular mechanisms and efficacy in in vivo models.

In contrast, WBE promoted growth in HepG2 cells, highlighting the variability in antioxidant responses across cancer types. This phenomenon may stem from the liver’s natural

exposure to antioxidants and its robust detoxification mechanisms, which make HepG2 cells more adaptable to antioxidant-induced stress [37–39]. Liver enzymes like cytochrome P450 can oxidize toxins, increasing their reactivity, where molecules such as glutathione attach to these reactive intermediates, and rendering them water-soluble for excretion [40]. Additionally, WBE's interaction with adhesion molecules or the extracellular matrix could account for the observed increase in spheroid dissociation time [41]. Similar findings in other cancer models suggest that antioxidants can modulate adhesion molecule expression, altering cellular dynamics [42,43]. The differential response between HepG2 and SW480 cells underscores the importance of cell-type specificity in antioxidant-based treatments. While WBE promotes growth in liver cancer cells, its ability to modulate oxidative stress and cellular behavior highlights its potential for therapeutic applications, provided its effects are carefully managed in specific cancer contexts.

In HeLa spheroids, WBE exhibited neither cytotoxicity nor significant morphological changes during the 4-day exposure. This lack of effect may result from cervical cancer cells' enhanced tolerance to oxidative stress, supported by high endogenous antioxidant enzyme levels, such as superoxide dismutase and catalase [44,45]. Additionally, concentration and exposure duration may have been insufficient to elicit cytotoxicity, suggesting that HeLa cells may require higher doses or longer exposure to reveal any potential effects. The structural complexity of the 3D spheroid culture model likely contributes to the observed resistance, as the cell-cell and cell-matrix interactions provide a more protective environment against oxidative challenges [46,47].

The unique responses of these cancer cell lines—cytotoxicity in SW480, growth promotion in HepG2, and no significant impact on HeLa—emphasize the complexity of antioxidant interactions with cancer cells. Factors such as cellular redox state, antioxidant defense mechanisms, and tissue origin must be considered when evaluating potential therapeutic

applications. WBE's selective effects highlight its promise for targeted cancer therapies, although further research is necessary to elucidate its mechanisms and optimize its therapeutic potential. Possible batch variability of wheat bran might be a limitation of this research. Investigating additional cancer cell lines and exploring the impact of dose and exposure duration will be critical next steps.

Chapter 5 - Conclusions

This study provides comprehensive insights into the effects of WBE on SW480, HepG2, and HeLa cancer cell lines within a 3D-embedded PGS matrix system. WBE exhibited selective effects, inhibiting growth in SW480 colon cancer cells through oxidative stress-induced apoptosis, promoting growth in HepG2 liver cancer cells likely due to their robust detoxification mechanisms, and having no significant impact on HeLa cervical cancer cells. These findings highlight the complexity of antioxidant interactions with cancer cells and underscore WBE's potential for targeted, personalized cancer therapies. Further research is necessary to elucidate the underlying molecular mechanisms, optimize dosing strategies, and evaluate its efficacy in *in vivo* models. Additionally, exploring WBE's synergy with conventional chemotherapies could provide valuable insights into combination treatments that enhance cancer therapy outcomes. This approach may offer synergistic effects tailored to specific cancers, such as augmenting chemotherapy efficiency in colon cancer or mitigating toxicity in liver cancer, thereby advancing personalized and more effective treatment strategies.

References

1. Akbari, B.; Baghaei-Yazdi, N.; Bahmaie, M.; Mahdavi Abhari, F. The Role of Plant-Derived Natural Antioxidants in Reduction of Oxidative Stress. *BioFactors* **2022**, *48*, 611–633.

2. Faraoni, P.; Laschi, S. Bioactive Compounds from Agrifood Byproducts: Their Use in Medicine and Biology. *Int J Mol Sci*. **2024** May 26;25(*11*):5776. doi: 10.3390/ijms25115776.

3. Li, C.; Wu, W.; Tilley, M.; Chen, R.; Sun, X.S.; Wang, W.; Li, Y. In Vitro Antioxidant Properties of Wheat Bran Extracts and Their Inhibitory Effects on Collagenase, Elastase, and Hyaluronidase. *ACS Food Science and Technology* **2024**, *4*, 1960–1966, doi:10.1021/acsfoodscitech.4c00310.

4. Shang, X.L.; Liu, C.Y.; Dong, H.Y.; Peng, H.H.; Zhu, Z.Y. Extraction, Purification, Structural Characterization, and Antioxidant Activity of Polysaccharides from Wheat Bran. *J Mol Struct* **2021**, 1233, doi:10.1016/j.molstruc.2021.130096.

5. Liguori, I.; Russo, G.; Curcio, F.; Bulli, G.; Aran, L.; Della-Morte, D.; Gargiulo, G.; Testa, G.; Cacciatore, F.; Bonaduce, D.; et al. Oxidative Stress, Aging, and Diseases. *Clin Interv Aging* **2018**, *13*, 757–772.

6. Kaur, A.; Yadav, M.P.; Singh, B.; Bhinder, S.; Simon, S.; Singh, N. Isolation and Characterization of Arabinoxylans from Wheat Bran and Study of Their Contribution to Wheat Flour Dough Rheology. *Carbohydr Polym* **2019**, *221*, 166–173, doi:10.1016/j.carbpol.2019.06.002.

7. Dupoiron, S.; Lameloise, M.L.; Bedu, M.; Lewandowski, R.; Fargues, C.; Allais, F.; Teixeira, A.R.S.; Rakotoarivonina, H.; Rémond, C. Recovering Ferulic Acid from Wheat Bran Enzymatic Hydrolysate by a Novel and Non-Thermal Process Associating Weak Anion-Exchange and Electrodialysis. *Sep Purif Technol* **2018**, *200*, 75–83, doi:10.1016/j.seppur.2018.02.031.

8. Ye, Z.W.; Zhang, J.; Townsend, D.M.; Tew, K.D. Oxidative Stress, Redox Regulation and Diseases of Cellular Differentiation. *Biochim Biophys Acta Gen Subj* **2015**, *1850*, 1607–1621.

9. Kruk, J.; Aboul-Enein, H.Y. Reactive Oxygen and Nitrogen Species in Carcinogenesis: Implications of Oxidative Stress on the Progression and Development of Several Cancer Types. *Mini-Reviews in Medicinal Chemistry* **2017**, *17*, doi:10.2174/1389557517666170228115324.

10. Kumari, S.; Badana, A.K.; Murali Mohan, G.; Shailender, G.; Malla, R.R. Reactive Oxygen Species: A Key Constituent in Cancer Survival. *Biomark Insights* **2018**, 13.

11. Jelic, M.D.; Mandic, A.D.; Maricic, S.M.; Srdjenovic, B.U. Oxidative Stress and Its Role in Cancer. *J Cancer Res Ther* **2021**, *17*, 22–28.

12. Stavely, R.; Nurgali, K. The Emerging Antioxidant Paradigm of Mesenchymal Stem Cell Therapy. *Stem Cells Transl Med* **2020**, *9*, 985–1006.

13. Islam, M.R.; Akash, S.; Rahman, M.M.; Nowrin, F.T.; Akter, T.; Shohag, S.; Rauf, A.; Aljohani, A.S.M.; Simal-Gandara, J. Colon Cancer and Colorectal Cancer: Prevention and Treatment by Potential Natural Products. *Chem Biol Interact* **2022**, 368.

14. Esmeeta, A.; Adhikary, S.; Dharshnaa, V.; Swarnamughi, P.; Ummul Maqsummiya, Z.; Banerjee, A.; Pathak, S.; Duttaroy, A.K. Plant-Derived Bioactive Compounds in Colon Cancer Treatment: An Updated Review. *Biomedicine and Pharmacotherapy* **2022**, 153.

15. Unnikrishnan Meenakshi, D.; Narde, G.K.; Ahuja, A.; Al Balushi, K.; Francis, A.P.; Khan, S.A. Therapeutic Applications of Nanoformulated Resveratrol and Quercetin Phytochemicals in Colorectal Cancer—An Updated Review. *Pharmaceutics* **2024**, 16.

16. Arzumanian, V.A.; Kiseleva, O.I.; Poverennaya, E. V. The Curious Case of the HepG2 Cell Line: 40 Years of Expertise. *Int J Mol Sci* **2021**, 22.

17. Cristani, M.; Citarella, A.; Carnamucio, F.; Micale, N. Nano-Formulations of Natural Antioxidants for the Treatment of Liver Cancer. *Biomolecules* **2024**, 14.

18. Casas-Grajales, S. Antioxidants in Liver Health. *World J Gastrointest Pharmacol Ther* **2015**, *6*, 59, doi:10.4292/wjgpt.v6.i3.59.

19. Silva, G.Á.F.; Nunes, R.A.L.; Morale, M.G.; Boccardo, E.; Aguayo, F.; Termini, L. Oxidative Stress: Therapeutic Approaches for Cervical Cancer Treatment. *Clinics* **2018**, 73.

20. Ono, A.; Koshiyama, M.; Nakagawa, M.; Watanabe, Y.; Ikuta, E.; Seki, K.; Oowaki, M. The Preventive Effect of Dietary Antioxidants on Cervical Cancer Development. *Medicina (Lithuania)* **2020**, *56*, 1–12.

21. Wu, T.M.; Liu, S.T.; Chen, S.Y.; Chen, G.S.; Wu, C.C.; Huang, S.M. Mechanisms and Applications of the Anti-Cancer Effect of Pharmacological Ascorbic Acid in Cervical Cancer Cells. *Front Oncol* **2020**, 10, doi:10.3389/fonc.2020.01483.

22. Edmondson, R.; Broglie, J. J.; Adcock, A. F.; Yang, L. Three-Dimensional Cell Culture Systems and Their Applications in Drug Discovery and Cell-Based Biosensors. *Assay and Drug Development Technologies* **2014**, 12(*4*), 207–218.

23. Jensen, C.; Teng, Y. Is It Time to Start Transitioning From 2D to 3D Cell Culture? *Frontiers in Molecular Biosciences* **2020**, *7*, 33.

24. Breslin, S.; O'Driscoll, L. Three-dimensional cell culture: the missing link in drug discovery. *Drug Discovery Today* **2013**, 18(*5-6*), 240–249.

25. Zhu, Y.; Conklin, D. R.; Chen, H.; Wang, L.; Sang, S. 5-Alk(en)ylresorcinols as the major active components in wheat bran inhibit human colon cancer cell growth. *Bioorganic & Medicinal Chemistry* **2011**, 19(*13*), 3973-3982.

26. Kim, M. J.; Yoon, W. J.; & Kim, S. S. Phytochemical compositions of immature wheat bran, and its antioxidant capacity, cell growth inhibition, and apoptosis induction through tumor suppressor gene. *Molecules* **2016**, 21(*10*), 1292.

27. Schindelin, J.; Arganda-Carreras, I.; Frise, E.; Kaynig, V.; Longair, M.; Pietzsch, T.; Preibisch, S.; Rueden, C.; Saalfeld, S.; Schmid, B.; et al. Fiji: An Open-Source Platform for Biological-Image Analysis. *Nat Methods* **2012**, *9*, 676–682.

28. Moon, J.C.; Hah, Y.S.; Kim, W.Y.; Jung, B.G.; Jang, H.H.; Lee, J.R.; Kim, S.Y.; Lee, Y.M.; Jeon, M.G.; Kim, C.W.; Cho, M.J. Oxidative stress-dependent structural and functional switching of a human 2-Cys peroxiredoxin isotype II that enhances HeLa cell resistance to H2O2-induced cell death. *Journal of Biological Chemistry* **2005**, 280(*31*), 28775-28784.

29. Islam, M.R.; Akash, S.; Rahman, M.M.; Nowrin, F.T.; Akter, T.; Shohag, S.; Rauf, A.; Aljohani, A.S.M.; Simal-Gandara, J. Colon Cancer and Colorectal Cancer: Prevention and Treatment by Potential Natural Products. *Chem Biol Interact* **2022**, *368*, 110170, doi:10.1016/j.cbi.2022.110170.

30. Lee, S.H.; Lee, H.S.; Lee, J.; Amarakoon, D.; Lou, Z.; Noronha, L.E.; Herald, T.J.; Perumal, R.; Smolensky, D. Polyphenol Containing Sorghum Brans Exhibit an Anti-Cancer Effect in Apc Min/+ Mice Treated with Dextran Sodium Sulfate. *Int J Mol Sci* **2021**, 22, doi:10.3390/ijms22158286.

31. García-Gutiérrez, N.; Maldonado-Celis, M.E.; Rojas-López, M.; Loarca-Piña, G.F.; Campos-Vega, R. The Fermented Non-Digestible Fraction of Spent Coffee Grounds Induces Apoptosis in Human Colon Cancer Cells (SW480). *J Funct Foods* **2017**, *30*, 237–246, doi:10.1016/j.jff.2017.01.014.

32. Safrida, S.; Budijanto, S.; Nuraida, L.; Priosoeryanto, B.P. Potency of Bioactive Compound of Rice Bran for Colon Cancer Prevention. *Jurnal Kesehatan Masyarakat* **2020**, *16*, 284–295, doi:10.15294/kemas.v16i2.21133.

33. Rao, S.; Chinkwo, K.; Santhakumar, A.; Johnson, S.; Blanchard, C. Apoptosis Induction Pathway in Human Colorectal Cancer Cell Line SW480 Exposed to Cereal Phenolic Extracts. *Molecules* **2019**, *24*, doi:10.3390/molecules24132465.

34. Esmeeta, A.; Adhikary, S.; Dharshnaa, V.; Swarnamughi, P.; Ummul Maqsummiya, Z.; Banerjee, A.; Pathak, S.; Duttaroy, A.K. Plant-Derived Bioactive Compounds in Colon

Cancer Treatment: An Updated Review. *Biomedicine and Pharmacotherapy* **2022**, *153*, 113384, doi:10.1016/j.biopha.2022.113384.

35. Lombardi, V.R.M.; Carrera, I.; Corzo, L.; Cacabelos, R. Role of Bioactive Lipofishins in Prevention of Inflammation and Colon Cancer. *Semin Cancer Biol* **2019**, *56*, 175–184, doi:10.1016/j.semcancer.2017.11.012.

36. Malcomson, F. C.; Willis, N. D.; Mathers, J. C. Is resistant starch protective against colorectal cancer via modulation of the WNT signalling pathway?. *Proceedings of the Nutrition Society* **2015**, 74(*3*), 282-291.

37. Han, K.H.; Hashimoto, N.; Fukushima, M. Relationships among Alcoholic Liver Disease, Antioxidants, and Antioxidant Enzymes. *World J Gastroenterol* **2016**, *22*, 37, doi:10.3748/WJG.V22.I1.37.

38. Ham, H.; Yoon, S.W.; Kim, I.H.; Kwak, J.; Lee, J.S.; Jeong, H. sang; Lee, J. Protective Effects of Unsaponifiable Matter from Rice Bran on Oxidative Damage by Modulating Antioxidant Enzyme Activities in HepG2 Cells. *LWT - Food Science and Technology* **2015**, *61*, 602–608, doi:10.1016/J.LWT.2014.12.047.

39. Alamri, Z.Z. The Role of Liver in Metabolism: An Updated Review with Physiological Emphasis. *Int J Basic Clin Pharmacol* **2018**, *7*, 2271, doi:10.18203/2319-2003.ijbcp20184211.

40. Blondet, N. M.; Messner, D. J.; Kowdley, K. V.; Murray, K. F. Mechanisms of hepatocyte detoxification. *In Physiology of the Gastrointestinal Tract*. Academic Press. **2018.** pp. 981-1001.

41. Jauković, A.; Abadjieva, D.; Trivanović, D.; Stoyanova, E.; Kostadinova, M.; Pashova, S.; Kestendjieva, S.; Kukolj, T.; Jeseta, M.; Kistanova, E.; et al. Specificity of 3D MSC Spheroids Microenvironment: Impact on MSC Behavior and Properties. *Stem Cell Rev Rep* **2020**, *16*, 853–875, doi:10.1007/s12015-020-10006-9.

42. Yildiz-Ozturk, E.; Saglam-Metiner, P.; Yesil-Celiktas, O. Lung Carcinoma Spheroids Embedded in a Microfluidic Platform. *Cytotechnology* **2021**, *73*, 457–471, doi:10.1007/s10616-021-00470-7.

43. Baster, Z.; Li, L.; Kukkurainen, S.; Chen, J.; Pentikäinen, O.; Győrffy, B.; Hytönen, V.P.; Zhu, H.; Rajfur, Z.; Huang, C. Cyanidin-3-Glucoside Binds to Talin and Modulates Colon Cancer Cell Adhesions and 3D Growth. *FASEB Journal* **2020**, *34*, 2227–2237, doi:10.1096/fj.201900945R.

44. Bhattacharjee, R.; Dey, T.; Kumar, L.; Kar, S.; Sarkar, R.; Ghorai, M.; Malik, S.; Jha, N.K.; Vellingiri, B.; Kesari, K.K.; et al. Cellular Landscaping of Cisplatin Resistance in Cervical Cancer. *Biomedicine & Pharmacotherapy* **2022**, *153*, 113345, doi:10.1016/J.BIOPHA.2022.113345.

45. Sevgi, K.; Tepe, B.; Sarikurkcu, C. Antioxidant and DNA Damage Protection Potentials of Selected Phenolic Acids. *Food and Chemical Toxicology* **2015**, *77*, 12–21, doi:10.1016/j.fct.2014.12.006.

46. Juarez-Moreno, K.; Chávez-García, D.; Hirata, G.; Vazquez-Duhalt, R. Monolayer (2D) or Spheroids (3D) Cell Cultures for Nanotoxicological Studies? Comparison of Cytotoxicity and Cell Internalization of Nanoparticles. *Toxicology in Vitro* **2022**, *85*, 105461, doi:10.1016/J.TIV.2022.105461.

47. Chai, Y.W.; Lee, E.H.; Gubbe, J.D.; Brekke, J.H. 3D Cell Culture in a Self-Assembled Nanofiber Environment. *PLoS One* **2016**, *11*, e0162853, doi:10.1371/JOURNAL.PONE.0162853.